International Journal of Thermophysics, Vol. 25, No. 2, March 2004 (© 2004)

The Use of Scanning Transitiometry to Investigate Thermodynamic Properties of Polymeric Systems over Extended T and p Ranges[1]

J.-P. E. Grolier,[2,3] F. Dan,[4] S. A. E. Boyer,[2,5] M. Orlowska,[6] and S. L. Randzio[6]

Scanning transitiometry is a newly developed technique in which one of the independent variables (p, V, or T) is scanned in the working cell of a very sensitive calorimeter while the other independent variable is kept constant. The change of the dependent variable is recorded simultaneously with the thermal effect associated with the process or the system under investigation. In the case of non-reacting systems which remain in a homogeneous state, both the mechanical and thermal outputs thus obtained give straightforward access to pairs of thermomechanical coefficients: α_p and κ_T, β_V and κ_T, C_p and α_p, C_V and β_V, depending on the pair of selected independent variables. When the system or the material sample goes through a chemical reaction or a phase change, the recorded information yields the corresponding heat and pVT characteristics. The working cell may also house an optical fiber probe for spectrophotometric *in situ* readings from UV to NIR, as well as injection and stirring devices permitting investigation of reacting systems. The actual operating ranges of current scanning transitiometers are $173\,\mathrm{K} < T < 673\,\mathrm{K}$ and $0.1 < p < 200$ MPa (or 400 MPa). With such equipment, bulk properties, phase transitions, and reactions (i.e., polymerization) can be advantageously studied. Selected examples, all dealing with polymeric systems (including biopolymers), are illustrated, namely, measurements of thermomechanical coefficients (thermal

[1] Paper presented at the Fifteenth Symposium on Thermophysical Properties, June 22–27, 2003, Boulder, Colorado, U.S.A.

[2] Laboratory of Thermodynamics of Solutions and Polymers, Blaise Pascal University, 24, Avenue des Landais, 63177-Aubière Cedex, France.

[3] To whom correspondence should be addressed. E-mail: j-pierre.grolier@univ-bpclermont.fr

[4] Department of Macromolecular Chemistry, Gh. Asachi Technical University, 71A Mangeron Avn., 6600-Iasi, Romania.

[5] French Institute of Petroleum, 69390 Vernaison, France.

[6] Institute of Physical Chemistry, Polish Academy of Science, ul. Kasprzaka 44/52, 01-224 Warsaw, Poland.

0195-928X/04/0300-0297/0 © 2004 Plenum Publishing Corporation

expansion, compressibility), characterization of transitions (fusion, crystallization, glass transition, gelatinization) and particle synthesis. All examples show that scanning transitiometry is a versatile technique that can be used to fully characterize thermophysical properties as well as the thermodynamic behavior of a large variety of systems and materials.

KEY WORDS: high or low temperature; high pressure; polymers; reaction calorimetry; scanning transitiometry.

1. INTRODUCTION

Research in polymer science continues to actively develop, producing numerous new elastomers, plastics, adhesives, coatings, and fibers. All of this new information is gradually being codified and unified with important new theories about the interrelationships among polymer structure, physical properties, and useful behavior. Thus, the ideas of thermodynamics, kinetics, and polymer chain structure work together to strengthen the field of polymer science [1].

Thermal methods of analysis have always been widely used in investigation of polymer properties, especially in the case of phase transitions. Phase transitions are very important in industrial practice; ignorance of a phase diagram, particularly at extreme conditions of pressure, temperature, and of chemical reactivity, is a limiting factor to the development of an industrial process, e.g., sol-gel transitions, polymerization under solvent near supercritical conditions, micro- and nanofoaming processes, etc. [2].

Calorimetry is a very versatile method to measure thermodynamic properties of substances and to follow phase change phenomena or chemical reactions. In most applications, calorimetry is carried out at constant pressure while the tracked phenomenon is observed on increasing or decreasing the temperature or reactant (either stepwise or at constant scanning rate) [3]. Many studies carried out at constant pressure (different from atmospheric pressure) were achieved by some authors [4–6] who investigated the influence of this state variable on the thermodynamic properties. Mostly these investigations were done under isothermal conditions and pressure changes were made step-wise [7, 8] or at a constant rate [9, 10].

The possibility of controlling the three most important thermodynamic variables (pVT) in calorimetric measurements makes it possible to perform simultaneous measurements of both thermal and mechanical contributions to the thermodynamic potential changes caused by the perturbation [11]. When referring to the Ehrenfest classification of transitions [12], one can easily understand how useful is the simultaneous recording of both mechanical and thermal derivatives in the analysis of transitions and interpretation of their nature, especially in complex systems. The simultaneous

determination of both thermal and mechanical contributions to the total change of thermodynamic potential not only leads to the complete thermodynamic description of the system under study, but also permits investigation of systems with limited stability or systems with irreversible transitions. This approach is also very useful in analyzing the course of a transition. By a proper external change of the controlling variable, the transition under investigation can be accelerated, impeded, or even stopped at any degree of its advancement and then taken back to the beginning, all with simultaneous recording of the heat and mechanical variable variations. This permits not only determination of the total changes of the thermodynamic functions for the transition but also allows analysis of their evolution along the advancement of the transformation. For this reason the technique was called scanning transitiometry [13]. The technique has been operated over wide pressure (up to 400 MPa) and temperature (173 to 673 K) ranges with the step-wise or the linear scan of the variable change. It has already been applied in investigations of systems of various nature such as liquid crystals, polymers, and dense liquids [14, 15]. Scanning transitiometry is particularly useful in determining pressure effects on various phase transitions in polymeric systems [6] and in measuring the thermomechanical coefficients in the vicinity of the critical point [7]. Recently, the technique was adapted to study transitions in polymeric systems under pressure of compressed supercritical fluids (SCF) [16]. Supercritical polymer transitiometry can be very easily adapted to investigation of other types of transitions, such as precipitation or crystallization from a supercritical phase. Scanning transitiometry should also be very helpful in teaching thermodynamics and materials science.

This paper presents selected results of investigations made with three scanning transitiometers that are all high pressure, constant mass calorimeters working in an isothermal or nonisothermal mode. This serves to illustrate performances and operating ranges of transitiometry applied to polymer science.

2. MEASUREMENTS

2.1. Materials

The three investigated polyethylenes were: low-density polyethylene, LDPE (Lotrex FC 1010) crystallinity 0.39; medium-density polyethylene, MDPE (Finantrene 3802) crystallinity 0.59; and high-density polyethylene, HDPE (Marlex 56020) crystallinity 0.73.

Poly(vinylidene fluoride), PDVF, used in the present study was kindly supplied by Total-Fina-Elf and had the following characteristics: $M_n = 113000$ and $M_w = 330000$.

The gases, 1,1-difluoroethylene, CH_2F_2 (+99%, Aldrich Chemical Company, Inc.), nitrogen (SAGA, France), and carbon dioxide (SAGA, France) were used without purification. The critical pressures and temperatures for CO_2 and $C_2H_2F_2$ are 7.38 MPa and 31 °C, and 5.82 MPa and 78.3 °C, respectively [17]. Wheat starch powder was from PROLABO, France, catalogue number 21 146 290 with amylose content $21.0 \pm 0.2\%$, lipid content $0.27 \pm 0.01\%$ and protein content $0.36 \pm 0.01\%$. In order to prepare a water emulsion or a paste, a given amount of demineralized and bidistilled water was added to a weighed sample of starch powder, and the mixture was carefully blended manually until a uniform mixture was obtained. The vulcanized rubber used in this study was a poly(butadiene-*co*-styrene) rubber with T_g of -26 °C at atmospheric pressure (determined with a Mettler Toledo DSC 821^e apparatus at 5 $K \cdot min^{-1}$).

2.2. Method

The new method presented here uses the basic principles of scanning transitiometry, previously described [13]. For the majority of selected examples the investigated polymer or polymer-based mixture was placed in the high pressure measuring cell surrounded by the calorimetric detector and a transition or a change in state was induced by a controlled variation of an independent variable (p, V, or T) while the other independent variable was kept constant. In all cases the variations of the dependent variable as well as the associated heat effects were simultaneously recorded as a function of time or of the scanned variable. Results of a transitiometric experiment are always a pair of simultaneous thermodynamic derivatives (thermal and mechanical) or a pair of thermomechanical coefficients [(α_p and κ_T); (β_V and κ_T); (C_p and α_p); or (C_V and β_V), depending on the selection of the pair of independent variables]. Except for part of Section 3.2. dealing with the influence of gas sorption, the reference cell was kept only as a thermal reference. In almost all cases the polymer sample was in direct contact with the pressure transmitting fluid (Hg, *n*-propanol, or supercritical fluid), the only exception concerns the study of biopolymer gelatinization where the wheat starch/water mixtures were encapsulated into a flexible, Pb or plastic, ampoule. For the low temperature investigations the mercury was replaced with *n*-propanol ($T_m = -97$ °C).

2.3. Instrument

A detailed scheme of the instruments used in this study and constructed according to the principle of scanning transitiometry is presented in Fig. 1. It consists of a calorimeter equipped with high-pressure vessels,

a pVT system, and LabVIEW-based virtual instrument (VI) software. Two cylindrical calorimetric detectors ($\varnothing = 17$ mm, $l = 80$ mm) each made from 622 thermocouples (chromel-alumel) are mounted differentially and connected to a nanovolt amplifier. The calorimetric detectors are placed in a metallic block, the temperature of which is directly controlled with a digital feedback loop of 22 bit resolution ($\sim 10^{-4}$ K), being part of the transitiometer software. The calorimetric block is surrounded by a heating-cooling shield. The temperature difference between the block and the heating-cooling shield is set to a constant value (5, 10, 20, or 30 K) and is controlled by an analogue controller. The temperature measurements, both absolute and differential, are performed with calibrated 100 Ω Pt sensors. The heaters are homogeneously embedded on the outer surfaces of both the calorimetric block and the heating-cooling shield. The whole assembly is placed in thermal insulation enclosed in a stainless steel body and placed on a stand, which permits moving the calorimeter up and down over the calorimetric vessels. When performing measurements near 273 K or below, dry air is pumped through the apparatus. A detailed description of the transitiometer is given elsewhere [18].

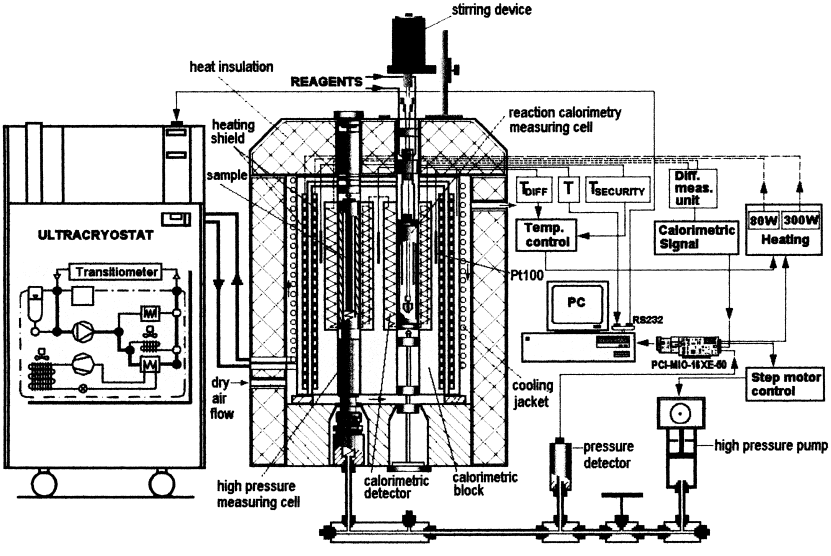

Fig. 1. Detailed scheme of a transitiometer installation for simultaneous and *in situ* analysis of thermal and volumetric properties of polymers at pressures up to 200 MPa and over the temperature range from 173 to 570 K. In this figure, for convenience two types of cells are shown (on the left-hand side the high-pressure cell and on the right-hand side the reaction cell).

3. RESULTS ON SELECTED SYSTEMS

To illustrate performance and advantages of scanning transitiometry in polymer science three main applications have been selected: (i) transitions of polymer systems under various constraints, including first-order phase transitions, glass transitions, and biopolymer gelatinization; (ii) polymer thermophysical properties and influence of gas sorption; and (iii) polymer particle synthesis.

3.1. Transitions of Polymer Systems Under Various Constraints

Different transitions of polymer systems under various constraints of pressure, temperature, and/or chemical reagents are reported hereafter.

3.1.1. First-Order Phase Transition

To begin with the simplest case, the first-order phase transition of semicrystalline polymers in the presence of a chemically inert fluid as a pressure-transmitting fluid is discussed. Mercury was preferred due to its chemical inertia and very good and well-known thermomechanical coefficients ($\alpha_p = 1.80 \times 10^{-4}\,K^{-1}$ and $\kappa_T = 0.40 \times 10^{-4}\,MPa^{-1}$). The polymer sample was always in intimate contact with the pressure transmitting fluid.

In the first example, Fig. 2a, the pressure effect on the melting/crystallization temperature of MDPE sample is illustrated. The isobaric temperature scans were performed at a rate of $0.833\,mK \cdot s^{-1}$. As can be seen in Fig. 2a, both fusion and crystallization are shifted toward higher temperatures with increasing pressure.

Figure 2b shows the corresponding rate of volume variations measured simultaneously in the same experiments. In Fig. 2 the melting temperature T_m and crystallization temperature T_{cr} have been obtained at the onset of the transition by the conventional method applied to the respective peaks. Taking as an example, the fusion at 200 MPa, the rates of variations with temperature of both volume and heat gave the same value of the melting temperature, i.e., 456.2 K. Variations of volume and of enthalpy in the same process were obtained by integration of curves from Figs. 2a and 2b, the corresponding values being $0.0573\,cm^3 \cdot g^{-1}$ and $-88.54\,J \cdot g^{-1}$, respectively [6]. The obtained value of $0.297\,K \cdot MPa^{-1}$ for $\Delta T_m/\Delta p$ (Clapeyron slope) is in fairly good agreement with the known literature values [16].

The scanning transitiometric technique was also adapted to work under supercritical conditions. In this case, the pressure transmitting fluid is the gas itself in a supercritical state. The polymer sample was contained

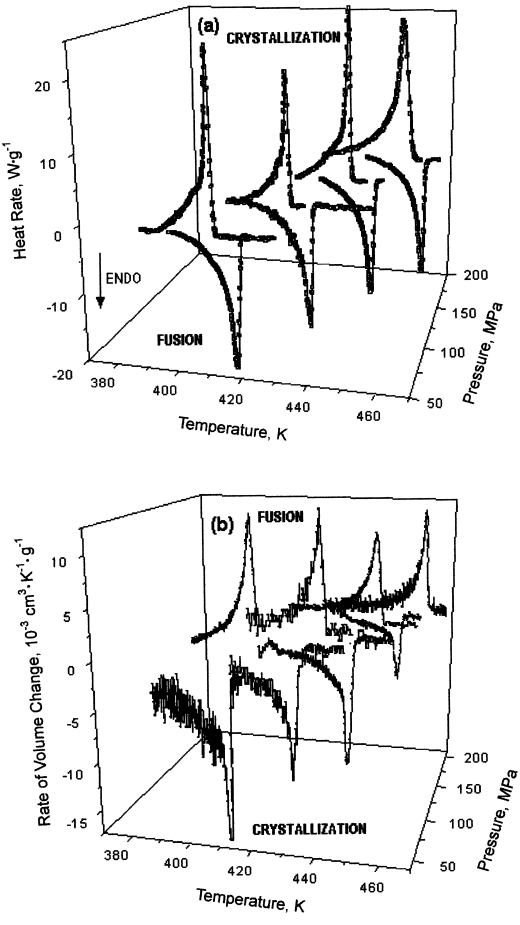

Fig. 2. Transitiometric traces obtained simultaneously *in situ* at various pressures for MDPE: (a) heat rate evolution during fusion and crystallization and (b) volume changes induced by the temperature scan.

in an open glass ampoule supported on a spring in the reaction cell (in order to be positioned in the central active part of the detector zone) and in direct contact with the pressurization fluid. The reaction vessel was connected to a pressure gauge and to the pump through a stainless steel high-pressure capillary tube; it can be also connected to a supercritical fluid tank for filling the fluid into the pump.

The systems PVDF/$C_2H_2F_2$ and PVDF/N_2 have been selected to illustrate this particular case. $C_2H_2F_2$ dissolves PVDF at high pressure and

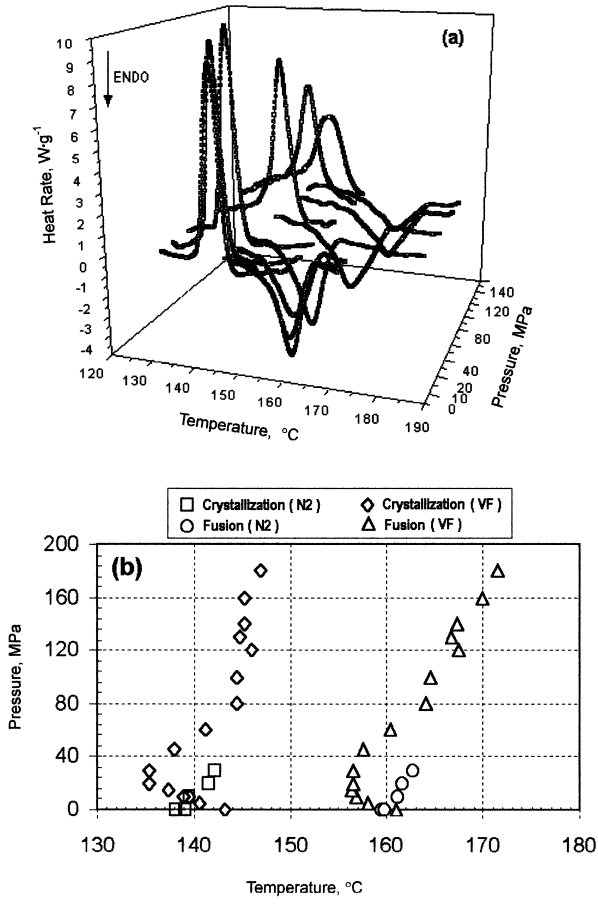

Fig. 3. Pressure effect on the temperature-induced and gas-assisted melting/crystallization of PVDF: (a) heat rate evolution during fusion and crystallization in the presence of supercritical $C_2H_2F_2$ (VF) and (b) partial *p-T* phase diagram for the PVDF-VF and PVDF-N_2 systems. Note the depression in the melting/crystallization temperature in the pressure range up to 30 MPa for the PVDF-VF system.

temperature, whereas nitrogen is inert with respect to the polymers and a comparative investigation is of interest. Figure 3a shows the influence of $C_2H_2F_2$ in the pressure range from 0.1 to 180 MPa on the melting and crystallization of PVDF. The width of the fusion peaks span is greater than the corresponding crystallization peaks independent of pressure, which is

not observed in the case of MDPE [see Fig. 2a]. The crystallization and fusion peaks broaden with increasing pressure, especially above 40 MPa, while the amplitude of the peaks concomitantly decreases.

Figure 3b shows the influence of $C_2H_2F_2$ and of N_2 on the temperatures of melting (T_m) and crystallization (T_{cr}). Clearly both temperatures increase with increasing N_2 pressure, similar to the effect observed on MDPE in Fig. 2. In the investigated range of pressure (0.1 to 30 MPa), the slope of the T_m-pressure and T_{cr}-pressure plots were $0.108 \pm 0.002\ K \cdot MPa^{-1}$ and $0.115 \pm 0.002\ K \cdot MPa^{-1}$, respectively. On the contrary, $C_2H_2F_2$ depresses the melting/crystallization point by sorption of gas in polymer up to 30 MPa. The antiplasticization effect of the hydrostatic pressure of $C_2H_2F_2$ is apparent above 30 MPa. Consequently, crystallization and melting temperatures are a compromise between the effect of hydrostatic pressure, which increases the transition temperatures of crystallization and fusion, and the solubility of the monomer ($C_2H_2F_2$) in the polymer-rich phase, which depresses these values.

3.1.2. Glass-Transition Temperature

The glass-transition temperature is also affected by pressure since an increased pressure causes a decrease in the total volume and an increase in T_g is expected based on the prediction of decreased free volume. This result is important in engineering operations such as molding or extrusions, when operation too close to T_g can result in a stiffening of the material.

Investigation of the glass transition of polymers under pressure is not a simple problem, especially in the case of elastomers whose T_g is usually well below ambient temperature. In this case the traditional pressure-transmitting fluid, mercury, must be replaced since its crystallization temperature is relatively high, i.e., 235.45 K. The choice of the replacement fluid is a challenge because it should be chemically inert with respect of the investigated sample (with respect to all its constituents). Also, values of its thermomechanical coefficients, compressibility, κ_T, and thermal expansivity, α_p, should be smaller than those of investigated samples. An additional difficulty in investigations of second-order type transformations is the relatively weak effect measured. It is well known that the amplitude of the heat flux at the glass transition T_g increases with the temperature scanning rate while the time constant of Tian–Calvet type calorimeters imposes temperature scan rates which are slow compared to typical DSC scan rates. However, with the use of an ultracryostat for scanning temperature, we have used the temperature program illustrated in the insert of Fig. 4a. This means that the temperature of the cooling liquid is lower than that of the calorimetric block during the stabilization periods (isothermal segments), and it is higher during the dynamic segment. In such a way, the scanning

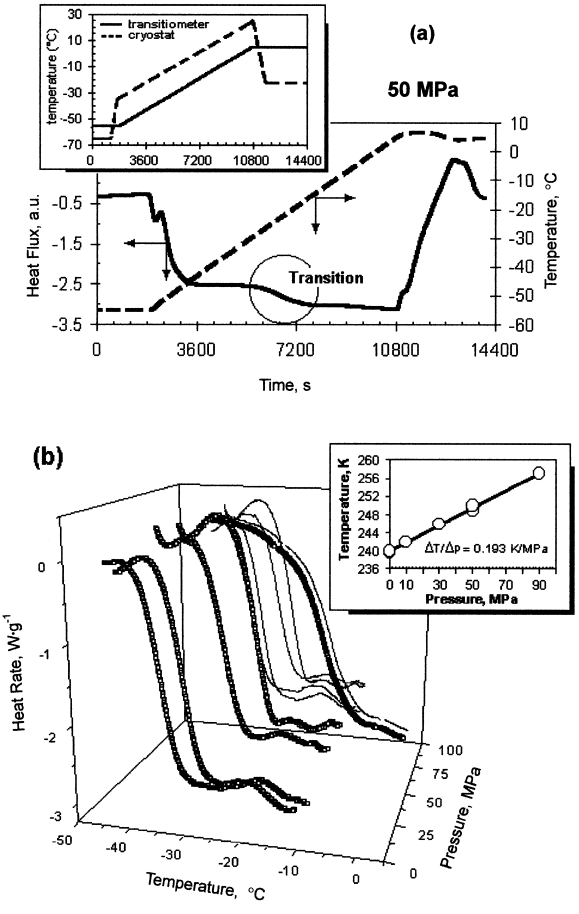

Fig. 4. Illustration of scanning transitiometry data for low-temperature, high-pressure investigation of a polymer glass transition: (a) experimental data obtained during an isobaric temperature scan at 50 MPa (styrene-butadiene rubber, SBR, sample mass = 1.56 g, scanning rate 0.4 $K \cdot min^{-1}$). In the insert the temperature program for the transitiometer (full line) and heat transfer fluid (dashed line) are depicted; (b) pressure effect on the glass transition temperature, T_g. The pressure coefficient of the glass transition temperature is given in the insert.

rate could be increased to 0.7 $K \cdot min^{-1}$ always keeping a minimal difference between target and real temperatures of the calorimetric block. Since the temperature gradient between the "heating fluid" and the calorimetric block was kept constant (20 K) the power uptake of the heating elements was quasi-constant, so the interference of sudden changes of power uptake

on the calorimetric signal was avoided. The calorimetric response of a poly(butadiene-*co*-styrene) vulcanized rubber during isobaric scanning of temperature at 50 MPa with temperatures ranging from 218.15 to 278.15 K at 0.4 $K \cdot min^{-1}$ is illustrated in Fig. 4a.

Figure 4b shows the evolution of T_g at different pressures, at 0.25, 10, 30, 50, and 90 MPa. As is seen in the insert of this figure, T_g increases linearly with pressure with a slope of $0.193 \pm 0.002\ K \cdot MPa^{-1}$. It should be noted that T_g is expressed as the temperature corresponding to the peak of the first derivative of the heat flux (i.e., the inflection point of the heat flux).

3.1.3. Biopolymers Gelatinization

A fundamental understanding of the influence of processing on food products requires studies which elucidate how the physical properties of food materials vary as a function of conditions encountered in processing. The main processing variables are temperature, pressure, and water content. Temperature and water content have already been extensively used as variables in physicochemical investigation of food materials performed with various techniques. However, pressure has been used very seldom, especially in *in situ* studies [19, 20]. But there is no doubt that temperature and pressure have equivalent importance as thermodynamic variables. Apart from the direct relation to extruder processing conditions, there are several other reasons to measure the effect of pressure on a wide variety of bio-systems important in food science and industry. The most important argument is that one can separate the effects of volume and thermal energy changes, which appear simultaneously in temperature scanning experiments [21]. Molecular processes that alter the volume of the system are especially sensitive to pressure. Volume changes associated with biochemical processes can therefore be revealed using pressure as an experimental variable.

The performance of scanning transitiometry is demonstrated here with a novel *in situ* investigation of pressure effects on the phase transformations occurring during gelatinization of (wheat starch + water) emulsions. In this case the wheat starch/water mixture was placed in a small plastic pouch to separate it from the pressurizing fluid. As an example of the advantage of the technique, Fig. 5 presents results obtained in isobaric experiments by scanning temperature at 2.5 $mK \cdot s^{-1}$ (0.15 $K \cdot min^{-1}$) at pressures of 10 and 60 MPa, respectively, for a wheat starch–water emulsion at 56% water content. Two output signals are recorded simultaneously; the heat rate and the volume variation as a function of temperature (thermal expansion) are quantities expressed per gram of the investigated emulsion. The most important observation is that all the transitions recorded previously at a temperature scanning rate of 1 $K \cdot min^{-1}$ with

a high sensitivity DSC at atmospheric pressure [22] are also shown by the transitiometric traces in Fig. 5 performed under elevated pressures at a scanning rate of 2.5 $mK \cdot s^{-1}$ (0.15 $K \cdot min^{-1}$).

This means that the transitiometry is a development of previous techniques, which permits study of the pressure influence on the course of transitions previously observed at atmospheric pressure, i.e., to record simultaneously and *in situ*, independent information on the volume variations at those transitions. In this respect one can see in Fig. 5 that the volume variation at the main endothermic transition (**M**) is always negative over the pressure range investigated. One also can notice that the volume variations at the other transitions are rather small, while the general tendency of the volume over the whole temperature range is to rise considerably with temperature which can be associated with swelling of starch during gelatinization. The main endothermic transition (**M**) is shifted a bit to lower temperatures when pressure increases which is thermodynamically consistent with the negative volume variation for that transition. Opposite to the main endothermic transition, the pressure influence on both the

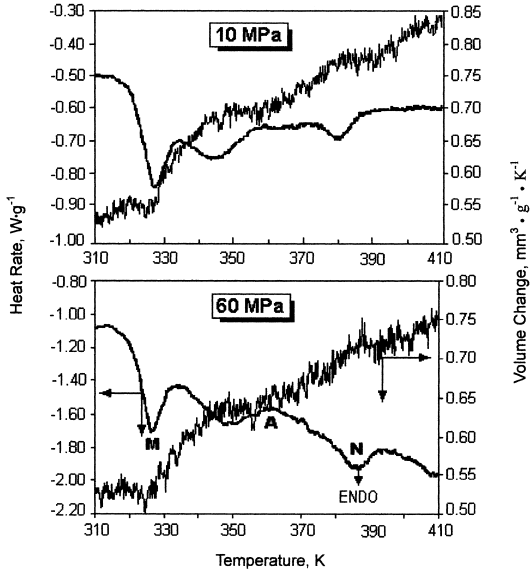

Fig. 5. Transitiometric traces obtained simultaneously and *in situ* at 10 and 60 MPa for a starch-water emulsion with 56.0 mass% water content. Note the volume contraction corresponding to the fusion peak M.

exothermic transformation (**A**) and the high-temperature small endothermic transition (**N**) is positive. Under a pressure of 10 MPa, the exothermic transformation starts at (348.6 ± 0.6) K and then is shifted by pressure to higher values at a rate of (38.9 ± 9.9) mK · MPa^{-1}, while the high-temperature endothermic transition starts at (382.7 ± 0.2) K and then is shifted by pressure to higher values at a rate of (96.1 ± 3.4) mK · MPa^{-1}.

3.2. Polymer Thermophysical Properties and Influence of Gas Sorption

Thermal expansion of polymers is a subject of considerable importance to both polymer scientists and engineers. In the first example, scanning transitiometry has been applied for measuring the isobaric thermal expansivities (α_p) of crystalline polyethylenes as a function of pressure up to 300 MPa at various temperatures. The measurements have been performed for polyethylenes with various degrees of crystallinity, χ_{cr}, at 302.6, 333.0, 362.6, and 393.0 K. These measurements were based on the Maxwell relation, which states that the isothermal pressure derivative of entropy is equal to but with opposite sign to the isobaric temperature derivative of volume. Thus, a calorimetric measurement of heat exchanged by a substance submitted to an isothermal pressure change leads to the determination of thermal expansion of the substance under investigation. Mercury was used as an inert hydraulic fluid in which the polymer sample was immersed. A detailed analysis of the working hypothesis and equations to access the isobaric thermal coefficients as well as the iterative procedure elaborated for derivation of α_p was given elsewhere [10]. The experimental requirements were further detailed [30] to show the basic principle and proper use of scanning transitiometry which is a more developed form of pressure-controlled calorimetry.

Isobaric thermal expansivities of polyethylenes of various densities follow the usual behavior of pressure and temperature dependence; α_p increases with temperature and decreases with pressure. Figure 6a–c illustrates the pressure effect on α_p for the three investigated polyethylenes. In all cases, the absolute magnitude of α_p and its strong dependence on both pressure and temperature are observed. As expected, the most sensitive, particularly with respect to temperature, was LDPE followed by MDPE and finally by HDPE. With increasing pressure, α_p decreases; the decrease is sharper for LDPE. Typically, α_p of polyethylenes of a given density shows the general trend to converge at high pressures.

In Fig. 6d the thermal expansitivities at 302.6 K are presented as a function of the degree of crystallinity of polyethylenes at various pressures. One can see a linear dependency of α_p with the degree of crystallinity. The straight lines in this figure have been obtained by least-squares fitting of

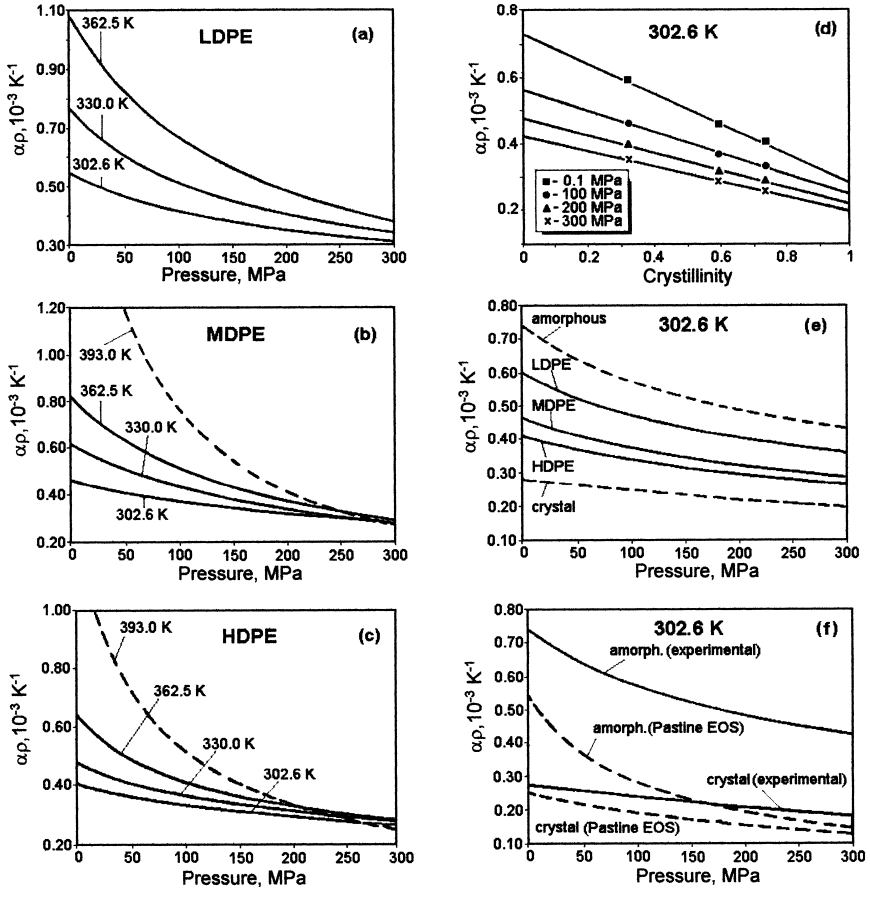

Fig. 6. Transitiometric investigation of the pressure effect on the isobaric thermal expansivities of various polyethylenes with different degrees of crystallinity. Effect of temperature on: (a) LDPE; (b) MDPE; and (c) HDPE. Extrapolation of the experimental data to the pure crystalline and amorphous phases at 302.6 K: (d) evolution of α_p with the crystallinity (points represent the experimental data and the lines were obtained by least squares fitting of data); (e) comparison between the experimental α_p and the predicted values for crystal and amorphous phases obtained by approximation from linear fitting of the experimental data; (f) α_p for amorphous and crystal phases of polyethylene obtained using scanning transitiometry and calculated from the Pastine theoretical equation.

the experimental data. From such linear approximations, α_p of both the amorphous phase and of the crystal phase could be derived. Figure 6e compares the thermal expansivities of low-, medium-, and high-density polyethylenes, with those predicted for fully amorphous and fully crystalline polyethylenes. At 302.6 K and 0.1 MPa the value of α_p for the

crystal phase is $2.81 \pm 0.04 \times 10^{-4}\,K^{-1}$; the corresponding literature value is $2.85 \times 10^{-4}\,K^{-1}$ [23]. Similar agreement was also observed between the present data for the crystal phase at atmospheric pressure at 333.0 K and the values calculated from the theoretical equation of state of Pastine [24, 25] for polyethylene. Similarly, at 302.6 K and at atmospheric pressure the agreement is also within a few percent [see Fig. 6f]. Disagreement in the case of the amorphous phase results most probably from the "liquid" contribution to the Pastine equation.

The second part of this subsection is devoted to the interactions between semicrystalline polymers, MDPE and PVDF, and one chemically active fluid, i.e., CO_2, at temperatures between T_g and T_m. Taking into account the differential principle of the instrument, two methods have been employed to investigate the interactions. In the first method the polymer sample is placed in the measuring cell where it is in contact with the fluid. The reference cell acts as a thermal reference, and an additional blank experiment (under identical conditions) is performed by replacing the polymer sample by an inert material of similar volume (i.e., metal, ceramic, and/or glass). The subtraction of the heat effects recorded from the blank experiment allows quantifying the thermal effect of polymer/fluid interactions. In the second method, employed here for the first time, a single experiment is performed in which the polymer sample is placed in the measuring cell while an inert sample of equal volume sits in the reference cell, both cells being connected to the pressure line. Under the assumption that the internal volumes of the two cells mounted differentially are exactly equal, during the fluid injection the work done inside the cells should also be exactly equal, but of opposite signs and thus should compensate completely. The measured calorimetric signal is in this case proportional to the thermal effect due to the polymer/fluid interactions.

Figure 7a shows some selected calorimetric responses for each of the two polymers at constant temperature (353.15 K) and under fast pressure changes. The pressure was step-wise varied in the range from 0.1 to 100 MPa with pressure jumps varying between 6 and 28 MPa. Despite the high compression in each step, the differential measured heat flux was very small, i.e., a few $mW \cdot cm^{-3}$ of polymer, which proves the correct thermal balance of the setup [30]. For both polymers the measured effects were exothermic, passing through a minimum in the pressure range from 10 to about 30 MPa. At low pressures, up to 20 MPa, the thermal heat flux is greater for the PVDF/CO_2 system. The baseline is achieved after about 1 hr in this range of pressure. Above 20 MPa the heat of interaction for MDPE/CO_2 exceeds the heat for PVDF/CO_2 system. However, the recorded heats become eventually identical at high pressures. Above 20 MPa the baseline is reached faster, usually in less than 30 min. The

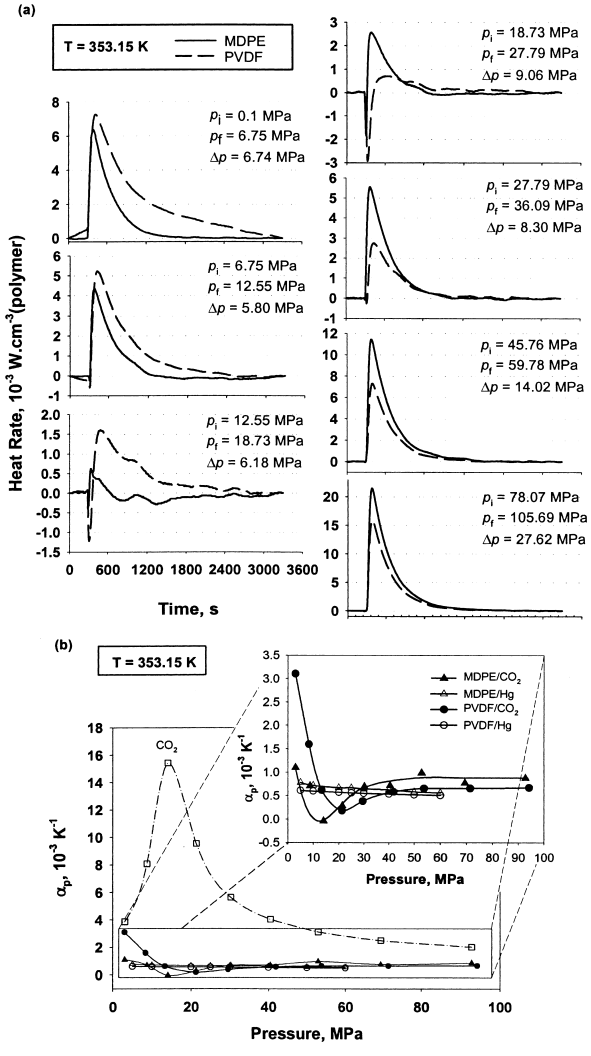

Fig. 7. High-pressure scanning transitiometry and gas sorption influence on thermophysical properties of polymers: (a) selected plots of the recorded heat rate during pressure jumps in the range from 0.1 to 100 MPa. Note that up to 20 MPa the enthalpy of interaction for the PVDF-CO_2 system is higher than that corresponding to the MDPE-CO_2 system; above this pressure the enthalpy change for the MDPE-CO_2 interaction is greater than that for PVDF-CO_2; (b) comparison between the isothermal expansivities of pure CO_2 and CO_2-pressurized MDPE, and CO_2-pressurized PVDF.

response time with blanks in both sides was shorter at the lowest pressures (< 30 MPa) and identical at highest pressures.

Under the assumption that there are no interactions between the reference (metal rod) and the fluid, and making use of Maxwell's equation one can get the isobaric thermal expansivities (α_p) of the saturated polymers at a given pressure. Figure 7b illustrates the comparative evolution of α_p in presence of two different fluids (actually used as hydraulic fluids), i.e., mercury-pressurized MDPE and PVDF, and CO_2-pressurized MDPE and PVDF. Around 20 MPa α_p of pure CO_2 is about one order of magnitude higher with the typical maximum usually observed in the vicinity of the critical point. On the contrary, α_p of the CO_2-saturated polymer (MDPE or PVDF) exhibits a shallow minimum at almost the same pressure, whereas in the case of Hg-pressurized polymers α_p shows a slight tendency to linearly decrease with pressure. To ascertain whether the above shallow minimum is either an experimental artifact or real behavior needs further investigation.

3.3. Polymer Particle Synthesis

In the case of polymer synthesis, the scanning transitiometer can be used as a reaction calorimeter, the advancement of a polymerization reaction being accurately monitored through rigorous control of the thermodynamic parameters. The differential configuration allows elimination of most of the systematic errors related to the experiment and/or heat transfer. The small thermal resistance makes it possible to work in a quasi-isothermal regime without power compensation, which is another major advantage of the present configuration. Results obtained from such measurements are to a large extent independent of the wetted surface or the stability of heat transfer, so that viscosity, minor changes in stirrer speed, and evaporation do not have to be taken into account here.

To gather additional information on a reaction, we developed a reaction cell which combines *in situ* UV/Vis/NIR spectrometry making use of a small optical probe coupled to a miniaturized spectrometer. In addition, the cell accommodates a stirrer and injection capillaries allowing different dosing profiles for one or two reactants.

The performance of this instrument is illustrated in the case of a process to which traditional reaction calorimetry was difficult to apply, such as precipitant polymerization, particularly the ultrafine polyamide (PA) particles synthesis by anionic polymerization of lactams in aprotic solvents. Anionic polymerization of lactams in organic solvents is a complex process. The most important steps in granular or powder polyamide

formation are as follows: initiation and growth of macromolecules in homogeneous medium, nucleation, phase separation and aggregation of the growing chains, solidification and, finally, polymer crystallization. All these events occur rapidly and partially overlap [26].

The polymerization occurs by the activated monomer mechanism, which supposes a two-step propagation mechanism involving the acylation of the lactam anion (NaL) by the *N*-acyllactam end-group of the growing chain followed by a fast proton-exchange with the monomer. The net result of each propagation step is the incorporation of a monomer unit into the polymer chain and the regeneration of the two active species [27].

In order to avoid the slow initiation step, the preformed *N*-acyllactams or their precursors (so called chain initiators, C.I.) are introduced in the system:

Initiation

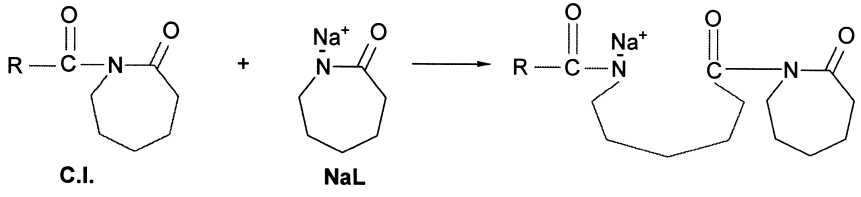

In the very strong basic medium the C.I. goes rapidly in side-reactions (Claisen condensation) and the polymerization is prematurely stopped [28]. Consequently, as long as monomer remains in the reaction medium, the polymerization can be continued simply by adding more chain initiator. In other words, the polymerization can be stopped and restarted by controlling the amount of C.I.

A detailed analysis of the strong temperature influence has been possible through measuring heat flux under isothermal conditions, at four successive temperatures, Fig. 8a or nonisothermal conditions, i.e., by temperature scanning, Fig. 8b. Noticeably, the shape of the curves representing the heat evolution with polymerization passes from two peaks at low temperature (up to 363 K) to a large shoulder [clearly seen in Fig. 9b] that diminishes around 375 K, and finally disappears at high temperature (above 393 K). The area of the first peak is not influenced by temperature, but the area of the second one strongly increases with temperature, and consequently the monomer conversion also increases.

Using *in situ* Vis spectrometry (see Fig. 9) it was established that the first peak corresponds to the initiation reaction, i.e., between the two catalytic species (a very fast reaction), while the second one is the thermal contribution of the propagation reaction and of polymer crystallization

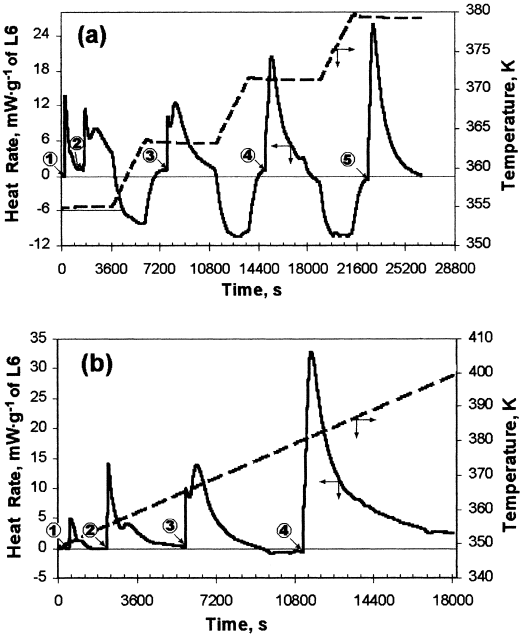

Fig. 8. Illustration of the temperature effect on the evolution of the heat released during anionic polymerization of caprolactam: (a) isothermal measurements at four temperatures (355, 363, 371, and 379 K); (b) non-isothermal measurements during four injections of chain initiator C.I. (temperature scan between 353 and 398 K at 0.12 $K \cdot min^{-1}$).

during the phase separation. Under nonisothermal conditions (temperature scanning) the same trend of heat evolution was observed, Fig. 8b. A 3D representation of the spectrometric signal evolution versus time at 363 K is given in Fig. 9a. It is worth noting the stability of light transmission in the homogenous medium and its sharp decrease at the beginning of phase separation (polymer precipitation). The combination of the two signals, Fig. 9b, clearly demonstrates that the second peak arises almost at the same time as the phase separation.

The main advantage of this process is related to the possibility of orienting it toward the preparation of powders with desired morphologies through a fine tuning of the synthesis parameters. To this goal it was demonstrated that one of the most convenient modalities is to continuously deliver the C.I. over a long period, Fig. 10a [29]. In the case of continuous

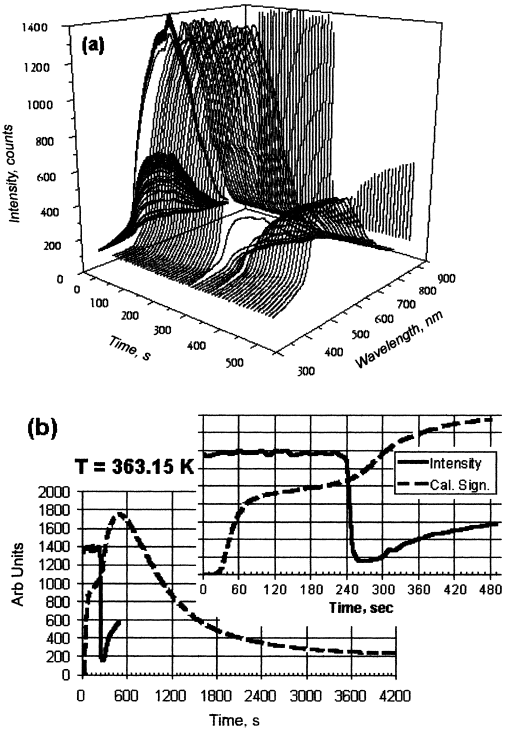

Fig. 9. Online combination of calorimetry and spectroscopy: (a) 3D plots of the evolution of the spectrometric signal during anionic polymerization of caprolactam; (b) simultaneous calorimetric and spectrometric signals recorded during polymerization at 363 K (the spectrometric signal was taken at 600 nm). Note the stability of the spectrometric signal before the phase separation and its sharp decrease at phase separation.

addition of C.I., three important indications are provided by the spectrometric data, Fig. 10b. The first one [I in Fig. 10b] concerns the period between the start of reaction and the beginning of polymer precipitation; it depends on temperature and on injection rate of C.I. The second one [II in Fig. 10b] is related to the particle size evolution with time (this is only qualitative information). Generally, after phase separation, the evolution of spectrometric signal runs parallel to the conversion. As is seen in Fig. 10b when one approaches the end of the process, the intensity of the spectrometric signal remains constant. Finally, the third piece of information (also

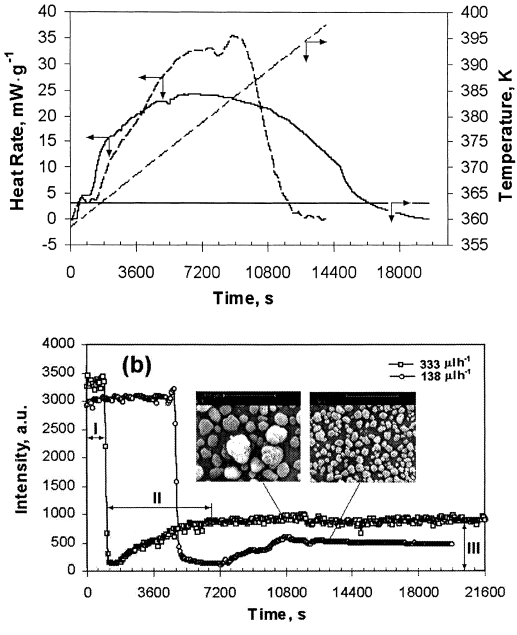

Fig. 10. Illustration of reaction calorimetry as a tool for process optimization: (a) controlled evolution of the heat rate by continuous addition of chain initiator C.I. over a pre-estabished period, here 4h with a rate of 60 $\mu L \cdot h^{-1}$ under isothermal (full lines) and non-isothermal conditions (dashed lines); (b) online qualitative development of particles and of their final size based on evolution of the spectrometric signal for different rates of feeding of C.I., i.e., 138 and 333 $\mu L \cdot h^{-1}$, respectively. The reaction temperature was 378 K, and the intensity of the spectrometric signal was recorded at 600 nm. In the inserts, the corresponding SEM micrographs of the obtained particles are given.

qualitative) refers to the average size of particles. It was proved by SEM [see inserts of Fig. 10b] that the average particle size is directly proportional to the final intensity of spectrometric signal [III in Fig. 10b].

4. CONCLUSION

In the field of polymer thermodynamics, new developments in calorimetric techniques, particularly in scanning transitiometry, have permitted investigations of three major applications. The first one deals with the

determination of thermophysical properties of polymers pressurized either by an incompressible inert fluid (mercury) or by highly compressible gases (like CO_2). The second one concerns the effect of pressure in the presence or the absence of gases on different phase transitions (fusion/crystallization and glass transitions) over wide temperature and pressure ranges. The third one illustrates how scanning transitiometry can be used as a versatile technique for one-line monitoring fine particles synthesis as well as particle size tuning.

ACKNOWLEDGMENTS

Financial support of Atofina and the French Institute of Petroleum is gratefully acknowledge. The transitiometers used in the present study were commercial instruments from BGR Ltd, Warsaw, Poland (for further information, contact randzio@ichf.edu.pl).

REFERENCES

1. L. H. Sperling, *Introduction to Physical Polymer Science*, 3rd edn. (Wiley, New York, 2001), p. xxix.
2. S. L. Randzio, *Thermochim. Acta* **355**:107 (2000).
3. P. Rollet and R. Bouaziz, *L'analyse thermique, Tome 1: Les changements de phase* (Gautier-Villars, Paris, 1972), p. 3577.
4. G. W. H. Höhne, *Thermochim. Acta* **332**:115 (1999).
5. Z. Zhang and Y. P. Handa, *Macromolecules* **30**:8505 (1997).
6. S. L. Randzio, *J. Therm. Anal. Cal.* **57**:165 (1999).
7. S. L. Randzio, J.-P. E. Grolier, and J. R. Quint, *High Temp.-High Press.* **30**:645 (1998).
8. P. Pruzan, L. TerMinassian, and A. Soulard, *High-Pressure Science and Technology* **1**:368 (1979).
9. S. L. Randzio, J.-P. E. Grolier, and J. Quint, *Rev. Sci. Instrum.* **65**:960 (1994).
10. Rodier-Renaud, S. L. Randzio, J.-P. E. Grolier, and J. R. Quint, *J. Polym. Sci. Part B: Polym. Phys.* **34**:1229 (1996).
11. S. L. Randzio, *Pure Appl. Chem.* **63**:1409 (1991).
12. P. Ehrenfest, *Proc. Kon. Akad. Wetensch.* **36**:153 (1933).
13. S. L. Randzio, *Chem. Soc. Rev.* **25**:383 (1996).
14. S. L. Randzio, *Thermochim. Acta* **300**:29 (1997).
15. S. L. Randzio, *J. Therm. Anal.* **48**:573 (1997).
16. S. L. Randzio and J.-P. E. Grolier, *Anal. Chem.* **70**:2327 (1998).
17. M. Loro, J. S. Lim, and M. A. McHugh, *J. Phys. Chem. B* **103**:2818 (1999).
18. S. L. Randzio, Ch. Stachowiak, and J.-P. E. Grolier, *J. Chem. Thermodyn.* **35**:639 (2003).
19. P. Rubens, J. Snauwaert, K. Heremans, and R. Stute, *Carbohydtrate Polym.* **39**:231 (1999).
20. P. Rubens and K. Heremans, *Biopolymers* **54**:524 (2000).
21. G. Weber and H. D. Drickamer, *Q. Rev. Biophys.* **16**:89 (1983).
22. S. L. Randzio, I. Flis-Kabulska, and J.-P. E. Grolier, *Macromolecules* **35**:8852 (2002).
23. M. Shen, W. N. Hansen, and P. C. Romo, *J. Chem. Phys.* **51**:425 (1969).

24. D. J. Pastine, *J. Appl. Phys.* **41**:5085 (1970).
25. D. J. Pastine, *J. Chem. Phys.* **49**:3012 (1968).
26. F. Dan and C. Vasiliu-Oprea, *Colloid Polym. Sci.* **276**:483 (1998).
27. H. Sekiguchi, in *Ring-Opening Polymerization*, Vol. 2, K. J. Iving and T. Saegusa, eds. (Elsevier, London, 1984), p. 833.
28. J. Stehlicek and J. Sebenda, *Eur. Polym. J.* **22**:769 (1986).
29. F. Dan and J.-P. E. Grolier, *Setaram News* **7**:i3–i4 (2002).
30. S. L. Randzio, *Thermochim. Acta* **398**:75 (2003).